CORTEX 52 (2014) 35–46

Available online at www.sciencedirect.com

ScienceDirect

Journal homepage: www.elsevier.com/locate/cortex

Research report

Multiple fMRI system-level baseline connectivity is disrupted in patients with consciousness alterations

Athena Demertzi[a,*,1], *Francisco Gómez*[a,b,1], *Julia Sophia Crone*[c,d], *Audrey Vanhaudenhuyse*[a], *Luaba Tshibanda*[e], *Quentin Noirhomme*[a], *Marie Thonnard*[a], *Vanessa Charland-Verville*[a], *Murielle Kirsch*[f], *Steven Laureys*[a,1] and *Andrea Soddu*[a,g,1]

[a] *Coma Science Group, Cyclotron Research Center & Neurology Department, University of Liège, Belgium*
[b] *Computer Science Department, Universidad Central de Colombia, Bogotá, Colombia*
[c] *Neuroscience Institute and Centre for Neurocognitive Research & Department of Neurology, Christian-Doppler-Clinic, Paracelsus Private Medical University, Salzburg, Austria*
[d] *Department of Psychology and Centre for Neurocognitive Research, University of Salzburg, Austria*
[e] *Department of Radiology, CHU University Hospital, University of Liège, Belgium*
[f] *Department of Anesthesiology, CHU University Hospital, University of Liège, Belgium*
[g] *Brain & Mind Institute, Physics & Astronomy Department, Western University, London, Ontario, Canada*

ARTICLE INFO

Article history:
Received 28 November 2012
Reviewed 10 April 2013
Revised 25 May 2013
Accepted 12 November 2013
Action editor Jordan Grafman
Published online 20 November 2013

Keywords:
Coma
fMRI
Resting state
Independent component analysis
Machine learning

ABSTRACT

Introduction: In healthy conditions, group-level fMRI resting state analyses identify ten resting state networks (RSNs) of cognitive relevance. Here, we aim to assess the ten-network model in severely brain-injured patients suffering from disorders of consciousness and to identify those networks which will be most relevant to discriminate between patients and healthy subjects.

Methods: 300 fMRI volumes were obtained in 27 healthy controls and 53 patients in minimally conscious state (MCS), vegetative state/unresponsive wakefulness syndrome (VS/UWS) and coma. Independent component analysis (ICA) reduced data dimensionality. The ten networks were identified by means of a multiple template-matching procedure and were tested on neuronality properties (neuronal *vs* non-neuronal) in a data-driven way. Univariate analyses detected between-group differences in networks' neuronal properties and estimated voxel-wise functional connectivity in the networks, which were significantly less identifiable in patients. A nearest-neighbor "clinical" classifier was used to determine the networks with high between-group discriminative accuracy.

Results: Healthy controls were characterized by more neuronal components compared to patients in VS/UWS and in coma. Compared to healthy controls, fewer patients in MCS and VS/UWS showed components of neuronal origin for the left executive control network, default mode network (DMN), auditory, and right executive control network. The "clinical" classifier indicated the DMN and auditory network with the highest accuracy (85.3%) in discriminating patients from healthy subjects.

* *Corresponding author*. Coma Science Group, Cyclotron Research Center & Neurology Department, Allée du 6 août n° 8, Sart Tilman B30, University of Liège, 4000 Liège, Belgium.
E-mail address: a.demertzi@ulg.ac.be (A. Demertzi).
[1] Authors contributed equally to this work.

http://dx.doi.org/10.1016/j.cortex.2013.11.005

Conclusions: FMRI multiple-network resting state connectivity is disrupted in severely brain-injured patients suffering from disorders of consciousness. When performing ICA, multiple-network testing and control for neuronal properties of the identified RSNs can advance fMRI system-level characterization. Automatic data-driven patient classification is the first step towards future single-subject objective diagnostics based on fMRI resting state acquisitions.

1. Introduction

Cumulative research on hemodynamic activity measured with functional MRI (fMRI) in resting state conditions suggests that the healthy brain can be organized in large-scale resting state networks (RSNs) of cognitive-behavioral relevance. More particularly, the default mode network (DMN), right and left executive control, auditory, salience, sensorimotor, cerebellum and three visual networks (lateral, medial, occipital) are consistently identified in healthy subjects (Damoiseaux et al., 2006; Laird et al., 2011; Smith et al., 2009) and show differential connectivity changes as the level of consciousness diminishes, such as in light (Horovitz et al., 2008) and deep sleep (Boly et al., 2012; Horovitz et al., 2009), anesthesia (Boveroux et al., 2010; Guldenmund et al., 2013; Martuzzi, Ramani, Qiu, Rajeevan, & Constable, 2010; Schrouff et al, 2011) and hypnosis (Demertzi et al., 2011; Hoeft et al., 2012; McGeown, Mazzoni, Venneri, & Kirsch, 2009). In clinical conditions, like dementia, coma and related disorders of consciousness, fMRI resting state investigations have mainly focused on the DMN which shows decreases in functional connectivity as a function of the level of consciousness (e.g., Buckner, Andrews-Hanna, & Schacter, 2008; Greicius, Srivastava, Reiss, & Menon, 2004; Norton et al., 2012; Vanhaudenhuyse et al., 2010). To date, a system-level characterization of fMRI baseline activity in patients with consciousness alterations is pending. Here, we aimed to assess the ten-cognitive-RSN model in severely brain-injured patients suffering from disorders of consciousness, namely in coma, vegetative state/unresponsive wakefulness syndrome (VS/UWS) and minimally conscious state (MCS). By means of an automatic data-driven approach, we further aimed to identify those RSNs, which were most relevant to discriminate unconscious and minimally conscious patients from healthy volunteers.

2. Methods

A widely-used methodology to investigate fMRI resting state functional connectivity is independent components analysis (ICA). ICA is a multivariate data-driven procedure, which evaluates the coherence of activity in multiple distributed voxels that are organized in maximally statistical independent components (Cole, Smith, & Beckmann, 2010). By this way, ICA is also able to isolate cortical connectivity maps from non-neuronal signals, such as head motion, cardiac pulsation and respiration (Beckmann, DeLuca, Devlin, & Smith, 2005). So far, ICA in severely brain-damaged patients was used to identify the DMN and adopted a two-step procedure: first, filtering low (<.007 Hz) and high (>.1 Hz) frequency signal fluctuations and then opting for a template-matching procedure, i.e., the IC which would best fit a predefined spatial template (representing the DMN) would be selected as the RSN of interest (e.g., Buckner et al., 2008; Greicius et al., 2004; Norton et al., 2012; Vanhaudenhuyse et al., 2010). We here recognize the methodological challenge when opting for a multiple RSN investigation in patients with severe brain damage. In particular, by using a single template-matching goodness-of-fit (GOF) procedure at a time, one runs the risk to erroneously identify a component as the RSN of interest. To better illustrate this issue, we consider the extreme case of a patient showing only one IC of neuronal origin. If merely using the single template-matching method, then this component would be assigned to the RSN we are investigating each time. Consequently, in cases of severely brain-injured patients, who are expected to show fewer components of neuronal origin, the identification of the accurate network can be jeopardized (Heine et al., 2012; Soddu et al., 2012). To identify multiple RSNs of interest, we here suggest: a) single-subject ICA decomposition, b) multiple template-matching procedure using binary integer programming and c) data-driven "neuronality" test for the selected RSNs. For further quantitative voxel-wise connectivity analyses, we propose that these are performed on those subjects and patients for whom the RSNs will be identified both in terms of spatial pattern and neuronal activity.

2.1. *Participants*

We prospectively assessed healthy volunteers and patients in coma, VS/UWS and MCS following severe brain damage studied at least 5 days after acute brain insult. Clinical examination was performed using the French version of the Coma Recovery Scale-Revised (CRS-R; Giacino, Kalmar, & Whyte, 2004; Schnakers et al, 2008). Exclusion criteria were contra-indication for MRI (e.g., presence of ferromagnetic aneurysm clips, pacemakers), MRI acquisition under sedation or anesthesia and large focal brain damage (>50% of total brain volume). Healthy participants were free of psychiatric or neurological history. The study was approved by the Ethics Committee of the Medical School of the University of Liège. Written informed consent to participate in the study was obtained from the healthy subjects and from the legal surrogates of the patients.

2.2. *fMRI data acquisition and preprocessing*

As in previous resting state paradigms classically performed by others (e.g., Beckmann et al., 2005; Greicius et al., 2004;

Raichle et al., 2001) and ourselves (e.g., Demertzi et al., 2011; Guldenmund et al., 2013; Soddu et al., 2012) we instructed the healthy volunteers to close their eyes, relax without falling asleep and refrain from any structured thinking (e.g., counting, singing etc.). The same instructions were given to patients but due to their cognitive and physical impairments, we could not fully control for a prolonged eye-closed yet awake scanning session. Nevertheless, patients were scanned under this condition as in previous work dealing with this clinical population (Boly et al., 2009; Vanhaudenhuyse et al., 2010).

In all patients and controls, functional MRI time series were acquired on a 3 T head-only scanner (Siemens Trio, Siemens Medical Solutions, Erlangen, Germany) operated with a standard transmit-receive quadrate head coil. Three hundred multislice T2*-weighted functional images were acquired with a gradient-echo echo-planar imaging sequence using axial slice orientation and covering the whole brain (32 slices; voxel size: $3 \times 3 \times 3$ mm^3; matrix size $64 \times 64 \times 32$; repetition time = 2,000 msec; echo time = 30 msec; flip angle = 78°; field of view = 192×192 mm^2). The three initial volumes were discarded to avoid T1 saturation effects. For anatomical reference, a high-resolution T1-weighted image was acquired for each subject (T1-weighted 3D magnetization-prepared rapid gradient echo sequence). Data preprocessing was performed using Statistical Parametric Mapping 8 (SPM8; www.fil.ion.ucl.ac.uk/spm). Preprocessing steps included realignment and adjustment for movement-related effects, coregistration of functional onto structural data, segmentation of structural data, spatial and functional normalization into standard stereotactic Montreal Neurological Institute (MNI) space, and spatial smoothing with a Gaussian kernel of 8 mm full width at half-maximum. Further motion correction was applied using ArtRepair toolbox for SPM (http://cibsr.stanford.edu/tools/ArtRepair/ArtRepair.htm), which corrects for small, large and rapid motions, noise spikes, and spontaneous deep breaths.

2.3. Extraction and identification of RSNs

The performed methodology is summarized in Fig. 1. First, single-subject ICA with 30 components was performed (Ylipaavalniemi & Vigario, 2008) using the infomax algorithm as implemented in the Group-ICA of fMRI toolbox (GIFT: http://icatb.sourceforge.net/). The component images (spatial maps) were calibrated to the raw data so the intensity values were in units of percent signal change (PSC) from the mean (Calhoun, Adali, Stevens, Kiehl, & Pekar, 2005). This fit was used to scale the component images into units, which reflect the deviation of the data from the mean, enabling a second-level random effects analysis to be performed (Calhoun, Adali, Pearlson, & Pekar, 2001). The ICs were then matched to the templates representative of the RSNs by means of a goodness-of-fit procedure. This method extends the single-template goodness-of-fit approach (e.g., Greicius et al., 2004) by quantifying the absolute PSC average of voxels falling in the template minus the PSC average of voxels outside the template. The templates for each RSN were selected by an expert (author AD) after visual inspection from a set of spatial maps resulting from Group ICA decomposition (30 components running GIFT) performed on 12 independently assessed controls (4 women, mean age = 21 years ± 3, scanned on a 3 T MR scanner using a gradient echo-planar sequence of axial slice orientation: 32 slices, voxel-size = $3.4 \times 3.4 \times 3.0$ mm^3, repetition time = 2,460 msec, echo time = 40 msec, flip angle = 90°, field of view = 220×220 mm^2). These templates were checked by another expert (author AS) for accuracy of structural labeling (for the full set of the 30 ICs and the selected templates see Supplementary Methods 1). Second, the multiple-template assignation procedure took place. In order to overcome potentially concurrent IC assignations to the same template, we introduced two physiologic constraints: (i) a template had to be assigned to one of the 30 ICs and (ii) an IC could be labeled as an RSN or not. The first constraint ensured

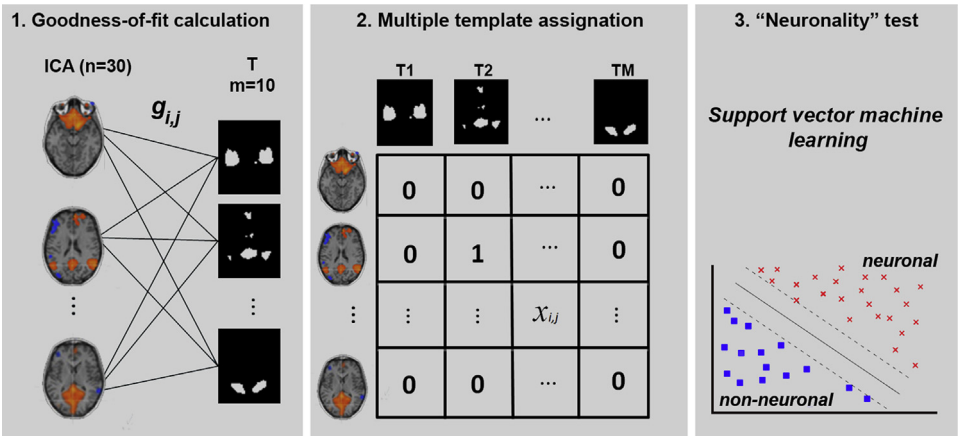

Fig. 1 – Illustrative methods summary for the extraction and identification of the RSNs. First, single-subject ICA was used to reduce fMRI data dimensionality into 30 independent components. Then, the goodness of fit ($g_{i,j}$) between the components and ten predefined spatial templates (T, representing the RSNs) was calculated. Second, the multiple-template assignation procedure referred to the concurrent component assignation by means of two constraints, where 1) an RSN template had to be assigned to one of the 30 independent components (column-wise) and 2) an independent component could be labeled as an RSN or not (row-wise). Finally, a binary automatic classification was used to separate the identified RSNs between those of neuronal and non-neuronal source (see Methods Section 2.3 and Supplementary Methods for more details).

that all templates would be assigned, given that the number of ICs was larger than the number of the templates. The second restriction forced a unique identification of each IC, which overcame the potentially concurrent component assignations. The multiple components labeling with assignation restrictions was formulated as a matching problem:

$$\max_x \sum_{i=1}^{N}\sum_{j=1}^{M} x_{i,j} g_{i,j}$$

$$\text{s. t.} \sum_{i=1}^{N} x_{i,j} = 1, 1 \le j \le M \quad (1)$$

$$\sum_{j=1}^{M} x_{i,j} \le 1, 1 \le i \le N \quad (2)$$

with $M = 10$ the number of different templates, $N = 30$ the number of ICs, $g_{i,j}$ the goodness of fit between the component i and the template j and $x_{i,j} \in \{0, 1\}$, an assignation binary variable indicating the match between the template j and the IC i. Hence, the couple between the template and IC with the highest global goodness of fit (taking into account all templates simultaneously) was eventually selected. The proposed optimization problem was solved by using binary integer programming (Grötschel & Holland, 1985). Third, for the discrimination between "neuronal" and "non-neuronal" ICs, we used a binary classification approach by means of support vector machine (SVM) classifier trained on 19 independently assessed healthy subjects. The feature, which was used for the training of the classifier was the fingerprints obtained from ICA decomposition ($n = 30$ components). The fingerprint is a feature vector which contains both spatial (i.e., degree of clustering, skewness, kurtosis, spatial entropy) and temporal information (i.e., one-lag autocorrelation, temporal entropy, power of five frequency bands: 0–.008 Hz, .008–.02 Hz, .02–.05 Hz, .05–.1 Hz, and .1–.25 Hz) and has been shown to discriminate neuronal from artifactual components (De Martino et al., 2007). For details on the training and selection of the classifier for the "neuronality test", see Supplementary Methods 2.

2.4. *Univariate analyses*

Mann–Whitney U tests assessed differences in the total number of neuronal components between the groups of controls, patients in MCS, VS/UWS and coma. Chi-square tests on contingency tables assessed differences in frequencies of neuronal RSNs between controls and patients. Results were considered significant at $p < .05$ corrected for multiple comparisons (Bonferroni correction).

Voxel-based between-groups comparisons (Holmes & Friston, 1998) were performed on the PSC IC maps of those healthy controls and patients for whom the RSNs were classified as "neuronal". A factorial design with three levels (controls, MCS, VS/UWS) was ordered for each RSN. A correction for non-sphericity was applied to account for potentially unequal variance across groups. In healthy controls, one-sided T contrast searched for the identification of the RSN of interest. Decreases in functional connectivity as a function of the level of consciousness (i.e., controls, MCS and VS/UWS) were assessed with exponential decay one-tailed T contrast, under the assumption that decreases in connectivity is more comparable among patients than healthy controls. Results were considered significant at $p < .05$ corrected for multiple comparisons at false discovery (FDR) for the whole brain volume.

2.5. *Multivariate analyses*

A nearest-neighbor "clinical" classifier was used to discriminate between healthy controls and all patients, between healthy controls and patients in VS/UWS and between healthy controls and patients in MCS. For each classification, three different kinds of inputs were used: first, a binary vector at the single-subject level representing the presence/absence (in terms of "neuronality"-"non-neuronality") of each of the ten RSNs (occurrence); second, a vector containing GOF values corresponding to each RSN without including information about neuronality (visual similarity); and third, a vector containing the product between the binary representation of neuronality and RSN GOF values (occurrence & visual similarity). For the classifier's validation, a leave-one-out cross validation was performed. Classification accuracy and accuracy-per-class were computed as measures of performance for the different classifications. In addition, a feature extraction method on the input vectors was also applied in order to determine those RSNs of discrimination relevance for each classification (Hall, 1999).

3. Results

Twenty-seven healthy volunteers (14 women; mean age: 47 ± 16 years; range: 20–72) and 53 patients with disorders of consciousness (24 in MCS, 24 in VS/UWS, 5 in coma; 20 women; mean age: 50 ± 18 years, range: 14–87; 34 of non-traumatic etiology of whom anoxic: 11, cerebrovascular accident: 12, hemorrhage: 9, seizure: 1, metabolic: 1; 17 of traumatic, and 2 of mixed etiology; 31 patients assessed in the chronic setting, i.e., ≥50 days post-insult) were included in the analysis Supplementary Table 1 summarizes the patients' demographic and clinical characteristics.

Fig. 2 summarizes the results of the "neuronality" classifier for all ICs in the groups of healthy controls and patients. For the ICs which were identified as RSNs, univariate analysis showed that the left executive control network, the DMN, the auditory and right executive control network were identified as neuronal in more healthy controls than patients; no between-group differences in neuronal ICs were observed for the rest of the RSNs (Fig. 3). For these four RSNs, functional connectivity was reproduced across healthy volunteers (Fig. 4, red color scale, Supplementary Table 2) and exponential voxel-wise contrasts resulted in reduced functional connectivity for most of the regions of each network (blue color scale, Table 1).

For the ICs which were identified as RSNs, multivariate analyses using the "clinical" classifier showed that information about occurrence of an RSN as neuronal or non-neuronal was of the highest accuracy to discriminate between healthy controls and all patients as well as between healthy controls and patients in VS/UWS (Table 2). The product vector occurrence * visual similarity was more successful for the

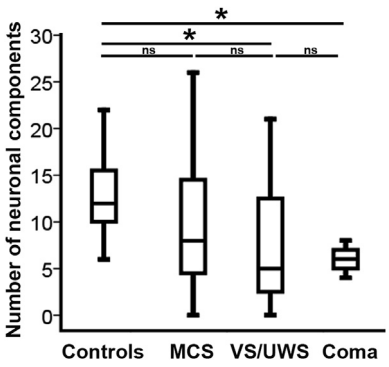

Fig. 2 – Across all independent components, healthy controls were characterized by more components of neuronal source compared to patients in VS/UWS and patients in coma; no differences in the number of neuronal components were identified between healthy controls and patients in MCS as well as between patients in MCS and VS/UWS. Boxplots represent medians with interquartile range and whiskers signify minimum and maximum values (*$p < .05$, Bonferroni correction, ns: non-significant).

discrimination between healthy controls and patients in MCS. Importantly for all classifications, the DMN and the auditory network were selected as the most discriminative features to distinguish between the healthy and clinical groups (Table 2, Supplementary Fig. 2).

4. Discussion

We here aimed to assess the ten RSN model, typically observed in healthy conditions (e.g., Damoiseaux et al., 2006; Laird et al., 2011; Smith et al., 2009), in severely brain-injured patients suffering from disorders of consciousness. By means of a multiple template-matching procedure and a "neuronality" test, we first found that patients with consciousness alterations exhibit fewer networks of neuronal origin compared to healthy subjects. The notion of reduced neural function in disorders of consciousness has been well documented by means of positron emission tomography (PET), with patients in VS/UWS showing 40–50% of normal metabolic values globally around the brain (Laureys, Owen, & Schiff, 2004). However, some polymodal areas, such as bilateral prefrontal regions, Broca's parieto-temporal, posterior parietal and precuneus, are systematically dysfunctional in pathologically unresponsive conditions (Kinney & Samuels, 1994; Laureys, Goldman, et al., 1999; Thibaut et al., 2012) and show functional recovery after patients regain consciousness (Laureys, Lemaire, Maquet, Phillips, & Franck, 1999). These results imply that not all brain regions contribute equally to sustain consciousness-related functions (Laureys, 2005). Under the assumption that our fMRI "neuronality" test classifier reflects, to some degree, neural function comparable to PET (Fig. 5), then our finding that not all RSNs were significantly disrupted in the patient sample align with such previous PET studies. Indeed, here, univariate analysis indicated that the DMN, auditory and the bilateral executive control networks were among the RSNs, which were less identifiable in patients compared to healthy controls and multivariate analyses confirmed so for the first two networks. Under healthy conditions, these four RSNs have been implicated in consciousness-related processing. More specifically, the bilateral executive control networks cover wide fronto-parietal areas. Resting state activity in these bilateral fronto-parietal cortices has been linked to performing externally imposed tasks (Corbetta & Shulman, 2002) but also relate to overt externally-oriented cognition during resting state (Fox, Corbetta, Snyder, Vincent, & Raichle, 2006). The DMN, on the other hand, has been associated with self-related internally directed cognition, including recollection of the past and thinking about the future, episodic memory retrieval and mind wandering (Buckner et al., 2008; D'Argembeau et al., 2008; Mason et al., 2007; Raichle et al., 2001). The bilateral fronto-parietal system and DMN were shown to have an anti-correlated function in the resting brain, where increased activity of one system parallels the reduced activity of the other (Fox et al., 2005; Fransson, 2005; Golland et al., 2007; Tian et al., 2007). We recently showed that such anticorrelated relationship has a behavioral correlate: subjective reports of increased "external awareness" (or perception of the environmental

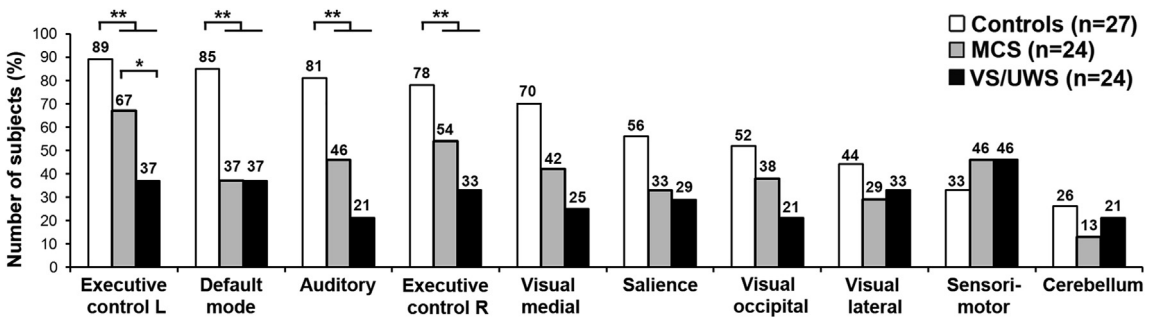

Fig. 3 – Across the ten RSNs, univariate analysis showed that fewer patients in MCS (gray bars) and VS/UWS (black bars) compared to healthy controls (white bars) exhibited the selected independent components (representing the left executive control, default mode, auditory, and right executive control network) as of neuronal origin ($p < .05$, Bonferroni correction). The left executive control network was characterized by neuronal source in more patients in MCS than in patients in VS/UWS (*$p < .05$, **$p < .001$).**

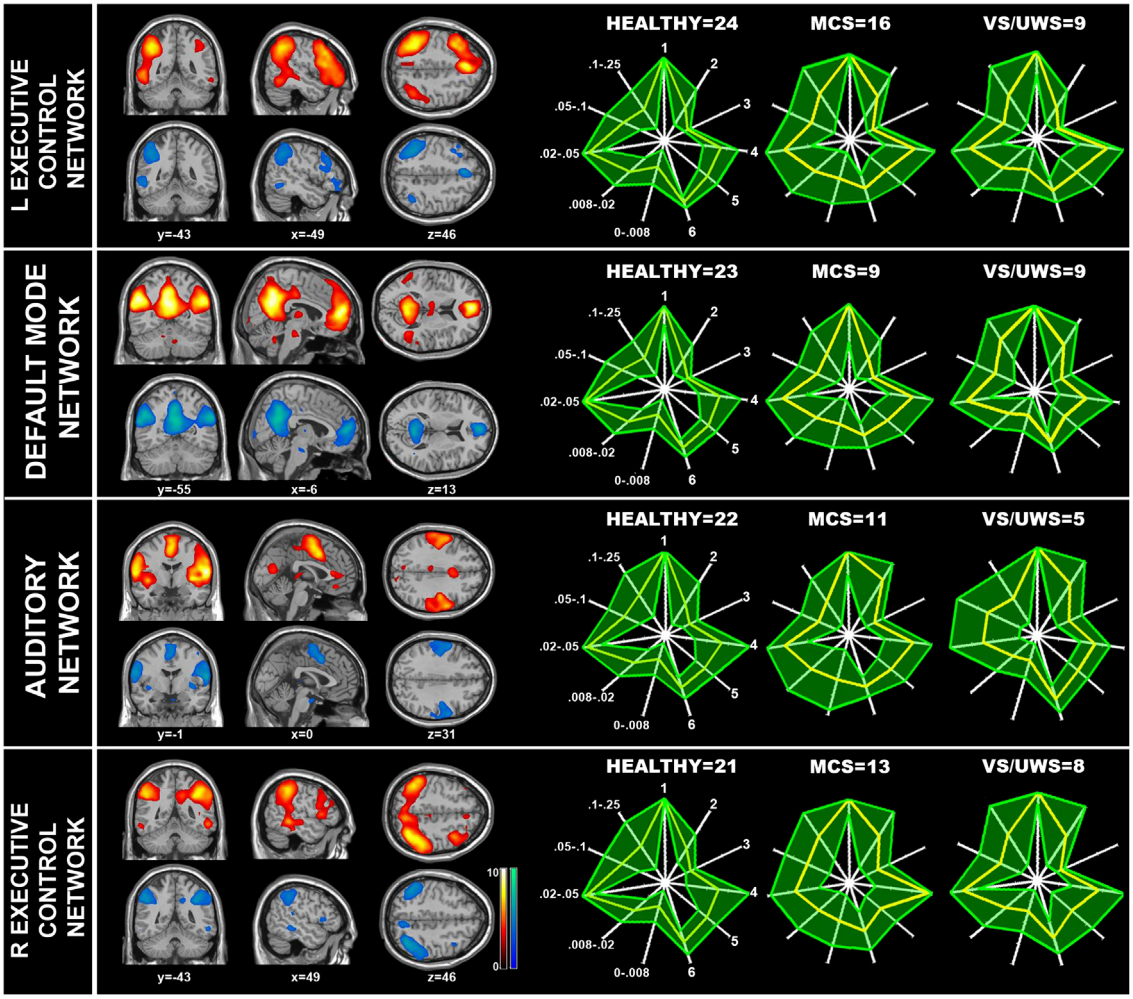

Fig. 4 – System-level fMRI resting state functional connectivity is reproduced across healthy controls (red color-scaled areas) and shows consciousness level-dependent decreases ranging from healthy subjects, to patients in MCS and VS/UWS (blue color-scaled areas). Group-level statistical inference was based on the independent components which were identified as the putative RSN by means of the multiple template-matching procedure and the "neuronality" test. As illustrated by the fingerprints, the included networks were characterized on average (yellow line) by neuronal origin (pick frequency at .02–.05 Hz; green areas represent one standard deviation above and below the group mean). Due to this selection procedure, some RSNs were not identified for some controls and patients (i.e., different group size per network). Statistical maps are thresholded at FDR for multiple comparisons $p < .05$ and are rendered on a structural T1 magnetic resonance template (x, y and z values indicate Montreal Neurological Institute coordinates of represented sections, neurological convention). Fingerprint labels: 1. degree of clustering, 2. skewness, 3. kurtosis, 4. spatial entropy, 5. one-lag autocorrelation, 6. temporal entropy.

stimuli through the senses) were linked to the activity of lateral frontoparietal areas; while subjective ratings of increased "internal awareness" (or self-related mentation) correlated with the activity in midline posterior and anterior areas (Vanhaudenhuyse et al., 2011). A legitimate question is to what degree reduced functional connectivity in these networks reflects diminished levels of conscious content in the absence of verbal reports. Hypnosis can work as an alternative experimental condition, wherein subjects remain fully responsive and can account for phenomenological modifications. Using this paradigm, we showed that functional connectivity of the external awareness system was hardly preserved under hypnosis and this cortical pattern was parallel to subjective reports of increased dissociation from the environment (Demertzi et al., 2011). Similar decreases in connectivity parallel to reduced awareness are also observed in sleep and pharmacologically-induced anesthesia (for a review see Heine et al., 2012). In the pathological condition of MCS, metabolic disruptions are shown for the internal (but not the external) awareness network, possibly accounting for their residual context-specific responsiveness of these patients to environmental demands (Thibaut et al., 2012). Our quantitative voxel-wise analysis indicated that consciousness level-dependent decreases in functional connectivity were observed in most

Table 1 – Peak voxels of the four RSNs showing reduced functional connectivity as a function of the level of consciousness, ranging from controls, patients in MCS and in VS/UWS.

Area (Brodmann area)	x	x	z	z value	p value
Left executive control network					
L Dorsolateral prefrontal cortex (46)	−54	20	28	4.61	.002
L Inferior frontal gyrus (47)	−54	38	−8	4.16	.004
L Middle frontal gyrus (9)	−54	20	28	4.61	.002
R Middle frontal gyrus (9)	54	17	31	3.41	.021
L Medial frontal gyrus (8)	−6	23	46	4.89	.001
L Inferior parietal lobe (40)	−36	−55	43	5.00	.001
R Inferior parietal lobe (40)	39	−58	46	3.94	.006
L Fusiform gyrus (37)	−57	−52	−5	4.48	.002
R Fusiform gyrus (37)	66	−37	−8	4.39	.002
R Primary visual cortex (17)	12	−88	10	3.15	.038
R Cerebellum	12	−82	−29	5.86	<.001
DMN					
Posterior cingulate cortex/Precuneus (31/7)	−3	−58	25	5.98	<.001
Anterior cingulate/medial prefrontal cortex (9/10/11)	−3	53	10	5.47	<.001
Midcingulate cortex (24)	0	−22	37	3.34	.011
L Angular gyrus (39)	−54	−67	25	6.54	<.001
R Angular gyrus (39)	54	−55	25	6.28	<.001
L Superior frontal gyrus (8)/middle frontal gyrus (6)	−36	14	52	4.89	<.001
L Inferior frontal gyrus (13)	−33	8	−11	3.64	.005
L Inferior parietal lobe (40)	−36	−34	55	3.57	.006
L Inferior (20)/middle temporal gyrus (21)	−57	−7	−20	4.48	<.001
R Inferior (20)/middle temporal gyrus (21)	63	−4	−26	5.12	<.001
L Parahippocampal gyrus (35)	−18	−25	−17	5.02	<.001
R Parahippocampal gurus (35)	24	−22	−23	3.73	.004
L Primary visual cortex (17)	−9	−97	1	3.83	.003
L Cerebellum	−30	−79	−35	4.39	<.001
R Cerebellum	30	−76	−35	4.81	<.001
Auditory network					
L Superior temporal gyrus (22)	−45	−31	22	3.400	.018
R Transverse temporal gyrus (41)	45	−31	13	3.590	.011
L Subcentral area (43)	−63	−13	19	4.97	.001
R Subcentral area (43)	63	−4	13	5.28	.001
L Postcentral gyrus (6)	−63	2	19	5.10	.001
R Postcentral gyrus (6)	60	−4	31	4.66	.001
L Superior orbital gyrus (11)	−15	62	−11	3.73	.008
Midcingulate cortex (24)	3	8	43	4.740	.001
Supplementary motor area (6)	−6	−10	64	4.88	.001
Precuneus (7)	−12	−55	64	4.05	.004
L Fusiform Gyrus (37)	−39	−76	−17	3.76	.008
Auditory network					
L Primary visual cortex (17)	−18	−64	4	3.200	.028
L Insula (13)	−39	−1	−5	4.070	.004
Thalamus	−3	−28	4	3.140	.032
Brainstem	6	−13	−29	3.60	.011
Right executive control network					
R Middle frontal gyrus (6)	33	11	55	3.83	.008
R Anterior prefrontal cortex (10)	36	53	−8	3.56	.015
R Inferior frontal gyrus (45)	51	17	4	3.58	.014
R Inferior parietal lobe (40)	36	−49	37	4.98	.001
L Inferior parietal lobe (40)	−42	−55	37	5.07	.001
R Middle temporal gyrus (20/21)	57	−43	−11	4.65	.001
Precuneus (7)	9	−70	34	4.23	.003
Posterior cingulate cortex (23)	6	−25	25	4.01	.005
Cerebellum	−9	−73	−23	4.63	.001

Significance values are corrected for multiple comparisons at FDR $p < .05$ (whole brain level).

regions of these four RSNs. Our results align with previous resting state fMRI studies in this patient population showing decreases in functional connectivity in the DMN (Norton et al., 2012; Soddu et al., 2012; Vanhaudenhuyse et al., 2010) and absent connectivity in brain death (Boly et al., 2009; Soddu et al., 2011). These data suggest that activity of such long-range cerebral systems, such as the DMN and the bilateral executive control networks, serve to a certain degree,

Table 2 – Results of the "clinical" classifiers.

Performance measures	Accuracy	TPR healthy	TPR patients	Selected RSNs
Healthy versus all patients				
Occurrence	85.3	.82	.875	Auditory, DMN
Occurrence & visual similarity	82.6	.70	.896	Auditory, DMN, visual lateral
Visual similarity	80	.78	.813	Auditory, DMN, ECNL, visual lateral
Healthy versus patients in MCS				
Occurrence & visual similarity	88.2	.89	.875	Auditory, DMN, ECNR
Occurrence	76.4	.82	.708	Auditory, DMN
Visual similarity	70.5	.78	.625	Auditory, DMN, ECNL
Healthy versus patients in VS/UWS				
Occurrence	86.2	.89	.833	Auditory, DMN
Visual similarity	74.5	.78	.708	Auditory, DMN
Occurrence & visual similarity	78.4	.78	.792	Auditory, DMN, ECNL

Occurrence: a vector containing information about the presence/absence of an RSN in terms of "neuronality"-"non-neuronality". Visual similarity: a vector containing goodness of fit values; Occurrence & visual similarity: a vector containing the product between occurrence and visual similarity. TPR: true positive rate; DMN, ECNL – executive control network left; ECNR: executive control network right.

conscious- and self-related cognition which is demolished in patients with consciousness alterations (Baars, 2005; Dehaene, Sergent, & Changeux, 2003; Dehaene & Changeux, 2011; also see Demertzi, Soddu, & Laureys, 2013; Demertzi, Vanhaudenhuyse, et al., 2013).

We further found that the auditory network was among the sensory RSNs, which was most consistently identified as neuronal in healthy controls and was significantly reduced in patients. The auditory system during rest has been associated with tasks related to audition (e.g., tone and pitch discrimination), music, and speech (Laird et al., 2011). We can only speculate why the auditory network was identified most frequently in healthy controls and not other sensory RSNs. It can be that because this system is the sole one being probed by relevant stimulation (i.e., background scanner noise), it can show higher connectivity compared to the visual and somatosensory RSNs, which do not receive any external stimulation. In any case, a less frequently identified auditory network in patients might account for their disrupted auditory perception. Indeed, patients in VS/UWS show an absent inter-regional connectivity between primary and associative auditory cortices (Laureys et al., 2000). On the contrary, patients in MCS show additional widespread activity including associative auditory cortices as well (Boly et al., 2004) allowing these patients for higher auditory function compared to patients in VS/UWS.

Finally, our "clinical" classifier indicated that the DMN and the auditory network elicited high accuracy (85.3%) in discriminating patients from healthy subjects. Further in our analysis, more patients in MCS showed ICs of neuronal activity in the left executive control network as compared to patients in VS/UWS. The left executive control network has been mainly linked to language-related processes (Laird et al., 2011; Smith et al., 2009), which seem preserved in MCS (Schiff et al, 2005) but not in VS/UWS patients (Coleman et al., 2007). Indeed, here the majority of the assessed MCS patients (16 out of 24, see Supplementary Table 1) showed command following when assessed with the CRS-R (Giacino, Kalmar, & Whyte et al., 2004). Command following was tested at the bedside by administering two commands, one object-related (e.g., look at the cup/look at the comb) and one non-object related (e.g., look up). If the patient followed both the object-related and the non-object related command in all eight administered trials (i.e., four trials per command), then the command following was scored as "consistent". If the patient showed three clearly discernible responses over the four trials on any of the object-related or non-object related command, command following was scored as "reproducible". It was recently shown that what differentiates MCS patients showing command following (MCS+) compared to those who only showed non-reflex behavior (MCS-) is preserved metabolism in the left hemisphere (Bruno et al., 2012). Although a discussion on the contribution of brain asymmetry to consciousness is beyond the scope of this article (e.g., Bruno et al., 2011; Ovadia-Caro et al., 2012), it seems nevertheless that the left hemisphere is needed to make elaborations above the level of minimal sensory consciousness (Turk, Heatherton, Macrae, Kelley, & Gazzaniga, 2003) which is preserved in MCS but lacking in VS/UWS patients.

From a methodological perspective, although the ten RSNs have been previously reported in healthy subjects in a reliable manner (e.g., Damoiseaux et al., 2006; Laird et al., 2011; Smith et al., 2009), our finding of less frequently identifiable RSNs in healthy volunteers could be explained by a number of factors. First, so far ICA resting state analysis in healthy controls was performed by using probabilistic (e.g., Beckmann et al., 2005) or Group ICA (e.g., Calhoun et al., 2001). What these methods have in common is individual data concatenation in space and/or time. Here, we recognize that to concatenate data deriving both from healthy controls and patients, we run the risk of mixing up brain signals of different properties. Hence, we feared that the subject-specific RSNs, which would be eventually returned (e.g., by means of dual regression) would be influenced by controls' data. To better account for inter-subject variability, we thus aimed for single-subject ICA and subsequent multiple-template matching. Following this approach, it is not surprising that healthy subjects do not present all RSNs within their own dataset. Further, in our adopted methodology we used a conservative approach for the identification of the RSNs, namely we decided to apply stricter criteria for the component selection by introducing the neuronal constraint. Our choice was justified by the wish to have comparable signal properties between the two populations and hence reduce between-group unknown variance as previously suggested when dealing with pathological groups (D'Esposito, Deouell, & Gazzaley, 2003). Due to that, the trained

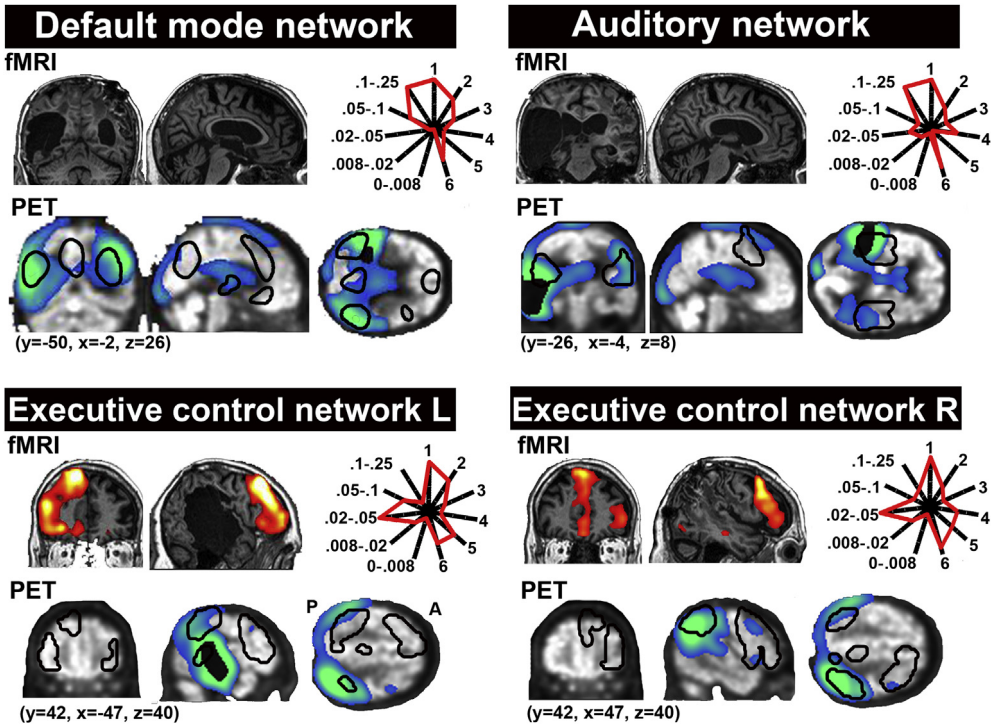

Fig. 5 – Upper panels: In a patient in VS/UWS, fMRI functional connectivity in the DMN and auditory network is excluded due to abnormal neuronal activity of the corresponding independent components (i.e., fingerprint time courses pick at very high frequency bands). Therefore, the network is considered absent. In the same patient, this disrupted fMRI connectivity parallels reduced metabolic activity (winter-colored maps) in most areas of each network (black contours) as measured with PET. Lower panels: For the executive control networks, preserved fMRI functional connectivity (warm-colored maps) in the anterior parts of each network coincides with preserved metabolism in these regions (i.e., empty black contours). This illustrative example implies a close link between the neuronality implicitly measured by fMRI and the neuronal function directly measured by PET. FMRI maps are rendered on the patients' structural T1 MRI and PET maps are superimposed on patient's computed tomography scan ($p < .05$ uncorrected; x, y and z values indicate Montreal Neurological Institute coordinates, neurological convention). Fingerprint labels: 1. degree of clustering, 2. skewness, 3. kurtosis, 4. spatial entropy, 5. one-lag autocorrelation, 6. temporal entropy. FMRI maps are superimposed on the patient's MRI scan.

"neuronality" classifier to separate components of neuronal and non-neuronal origin excluded those components characterized by atypical fingerprint features. Considering the lack of understanding whether and how an injured brain can constitute a whole "new" system instead of an "abnormal' one (He, Shulman, Snyder, & Corbetta, 2007), we recognize that our hypothesis on comparable neuronal function between controls and patients was strong. Nevertheless, we insisted on this neuronal control because in that way we could account for artifactual BOLD signal. Indeed, as shown by an illustrative example in Fig. 5, the selected neuronal ICs are tightly linked to cortical metabolism. Finally, the non-identification of some components as RSNs in the healthy control group could also be attributed to excessive motion in the scanner. Indeed, motion has been reported as a major source of artifact influencing intrinsic functional connectivity network measures; as such, subtly different levels of head motion can yield statistical maps, which can be mistaken for neuronal effects in other contexts (Van Dijk, Sabuncu, & Buckner, 2012). Here, although our healthy subjects moved less (mean speed index = .31 ± .12) compared to patients (mean speed index = .74 ± .49, $p < .001$) (Soddu et al., 2012), the number of total neuronal components correlated negatively with motion speed in controls (Kendall's tau = −.35, $p = .013$) but not in patients (Kendall's tau = −.078, ns). In other words, higher motion in healthy controls was associated with less frequently classified ICs as neuronal. Therefore, motion could have affected the fingerprint space in controls more than in patients, possibly because for controls motion is the main artifactual source affecting the quality of the BOLD signal (Van Dijk et al., 2012). In patients, excessive motion in the scanner can also lead to erroneous functional connectivity, although not to the same degree as in healthy subjects because in patients the BOLD signal is contaminated by many sources of noise due to the underlying neuropathology (D'Esposito et al., 2003). Indeed, we recently showed that in a brain dead patient an identified residual connectivity could be explained by motion artifacts (Soddu et al., 2011).

5. Conclusions

FMRI multiple-network connectivity is disrupted in severely brain-injured patients suffering from disorders of consciousness. When performing ICA, the identification of the "right" network may not be feasible due to structural and temporal

alterations in patients' BOLD signal. By multiple-network testing and controlling for neuronal properties of the identified RSN, we can advance fMRI system-level characterization. Automatic data-driven patient classifications based on fMRI resting state acquisitions are the first step towards single-subject objective diagnostics. The future challenge is to identify those fMRI-based features (at the single network or multiple-network level), which will promote diagnostic accuracy by correctly identifying true positives and true negative classes. We align with this network approach to the understanding of severe brain injury (Corbetta, 2012) and we foresee that the characterization of network spatiotemporal dynamics will further shed light on the patient-level cortical dysfunction.

Acknowledgments

This work was supported by the Belgian National Funds for Scientific Research (FNRS), tinnitus Prize 2011 (FNRS 9.4501.12), the European Commission, the James McDonnell Foundation, the European Space Agency, Mind Science Foundation, the French Speaking Community Concerted Research Action, the Belgian interuniversity attraction pole, the Public Utility Foundation "Université Européenne du Travail", "Fondazione Europea di Ricerca Biomedica" and the University and University Hospital of Liège. The authors have no conflicts of interest and no disclosures of financial interest to report.

Supplementary data

Supplementary data related to this article can be found at http://dx.doi.org/10.1016/j.cortex.2013.11.005.

REFERENCES

Baars, B. J. (2005). Global workspace theory of consciousness: toward a cognitive neuroscience of human experience. *Progress in Brain Research, 150*, 45–53.

Beckmann, C. F., DeLuca, M., Devlin, J. T., & Smith, S. M. (2005). Investigations into resting-state connectivity using independent component analysis. *Philosophical Transactions of the Royal Society of London. Series B, Biological Sciences, 360*(1457), 1001–1013.

Boly, M., Faymonville, M.-E., Peigneux, P., Lambermont, B., Damas, P., Del Fiore, G., et al. (2004). Auditory processing in severely brain injured patients: differences between the minimally conscious state and the persistent vegetative state. *Archives of Neurology, 61*(2), 233–238.

Boly, M., Perlbarg, V., Marrelec, G., Schabus, M., Laureys, S., Doyon, J., et al. (2012). Hierarchical clustering of brain activity during human nonrapid eye movement sleep. *Proceedings of the National Academy of Sciences, 109*(15), 5856–5861.

Boly, M., Tshibanda, L., Vanhaudenhuyse, A., Noirhomme, Q., Schnakers, C., Ledoux, D., et al. (2009). Functional connectivity in the default network during resting state is preserved in a vegetative but not in a brain dead patient. *Human Brain Mapping, 30*, 2393–2400.

Boveroux, P., Vanhaudenhuyse, A., Bruno, M.-A., Noirhomme, Q., Lauwick, S., Luxen, A., et al. (2010). Breakdown of within- and between-network resting state functional magnetic resonance imaging connectivity during propofol-induced loss of consciousness. *Anesthesiology, 113*(5), 1038–1053.

Bruno, M.-A., Fernandez-Espejo, D., Lehembre, R., Tshibanda, L., Vanhaudenhuyse, A., Gosseries, O., et al. (2011). Multimodal neuroimaging in patients with disorders of consciousness showing "functional hemispherectomy". *Progress in Brain Research, 193*, 323–333.

Bruno, M.-A., Majerus, S., Boly, M., Vanhaudenhuyse, A., Schnakers, C., Gosseries, O., et al. (2012). Functional neuroanatomy underlying the clinical subcategorization of minimally conscious state patients. *Journal of Neurology, 259*(6), 1087–1098.

Buckner, R. L., Andrews-Hanna, J. R., & Schacter, D. L. (2008). The brain's default network: anatomy, function, and relevance to disease. *Annals of the New York Academy of Sciences, 1124*, 1–38.

Calhoun, V. D., Adali, T., Pearlson, G. D., & Pekar, J. J. (2001). A method for making group inferences from functional MRI data using independent component analysis. *Human Brain Mapping, 14*(3), 140–151.

Calhoun, V. D., Adali, T., Stevens, M. C., Kiehl, K. A., & Pekar, J. J. (2005). Semi-blind ICA of fMRI: A method for utilizing hypothesis-derived time courses in a spatial ICA analysis. *NeuroImage, 25*(2), 527–538.

Cole, D. M., Smith, S. M., & Beckmann, C. F. (2010). Advances and pitfalls in the analysis and interpretation of resting-state FMRI data. *Frontiers in Systems Neuroscience, 4*(8).

Coleman, M. R., Rodd, J. M., Davis, M. H., Johnsrude, I. S., Menon, D. K., Pickard, J. D., et al. (2007). Do vegetative patients retain aspects of language comprehension? Evidence from fMRI. *Brain, 130*(10), 2494–2507.

Corbetta, M. (2012). Functional connectivity and neurological recovery. *Developmental Psychobiology, 54*(3), 239–253.

Corbetta, M., & Shulman, G. L. (2002). Control of goal-directed and stimulus-driven attention in the brain. *Nature Reviews Neuroscience, 3*(3), 201–215.

D'Argembeau, A., Feyers, D., Majerus, S., Collette, F., Van der Linden, M., Maquet, P., et al. (2008). Self-reflection across time: cortical midline structures differentiate between present and past selves. *Social Cognitive and Affective Neuroscience, 3*(3), 244–252.

D'Esposito, M., Deouell, L. Y., & Gazzaley, A. (2003). Alterations in the BOLD fMRI signal with ageing and disease: a challenge for neuroimaging. *Nature Reviews Neuroscience, 4*(11), 863–872.

Damoiseaux, J. S., Rombouts, S. A., Barkhof, F., Scheltens, P., Stam, C. J., Smith, S. M., et al. (2006). Consistent resting-state networks across healthy subjects. *Proceedings of the National Academy of Sciences, 103*(37), 13848–13853.

De Martino, F., Gentile, F., Esposito, F., Balsi, M., Di Salle, F., Goebel, R., et al. (2007). Classification of fMRI independent components using IC-fingerprints and support vector machine classifiers. *NeuroImage, 34*(1), 177–194.

Dehaene, S., & Changeux, J. P. (2011). Experimental and theoretical approaches to conscious processing. *Neuron, 70*(2), 200–227.

Dehaene, S., Sergent, C., & Changeux, J. P. (2003). A neuronal network model linking subjective reports and objective physiological data during conscious perception. *Proceedings of the National Academy of Sciences, 100*(14), 8520–8525.

Demertzi, A., Soddu, A., Faymonville, M.-E., Bahri, M.-A., Gosseries, O., Vanhaudenhuyse, A., et al. (2011). Hypnotic modulation of resting state fMRI default mode and extrinsic network connectivity. *Progress in Brain Research, 193*, 309–322.

Demertzi, A., Soddu, A., & Laureys, S. (2013). Consciousness supporting networks. *Current Opinion in Neurobiology, 23*(2), 239–244.

Demertzi, A., Vanhaudenhuyse, A., Bredart, S., Heine, L., Di Perri, C., & Laureys, S. (2013). Looking for the self in pathological unconsciousness. *Frontiers in Human Neuroscience, 7*, 538.

Fox, M. D., Corbetta, M., Snyder, A. Z., Vincent, J. L., & Raichle, M. E. (2006). Spontaneous neuronal activity distinguishes human dorsal and ventral attention systems. *Proceedings of the National Academy of Sciences of the United States of America, 103*(26), 10046–10051.

Fox, M. D., Snyder, A. Z., Vincent, J. L., Corbetta, M., Van Essen, D. C., & Raichle, M. E. (2005). The human brain is intrinsically organized into dynamic, anticorrelated functional networks. *Proceedings of the National Academy of Sciences, 102*(27), 9673–9678.

Fransson, P. (2005). Spontaneous low-frequency BOLD signal fluctuations: an fMRI investigation of the resting-state default mode of brain function hypothesis. *Human Brain Mapping, 26*(1), 15–29.

Giacino, J. T., Kalmar, K., & Whyte, J. (2004). The JFK Coma Recovery Scale-Revised: measurement characteristics and diagnostic utility. *Archives of Physical Medicine and Rehabilitation, 85*(12), 2020–2029.

Golland, Y., Bentin, S., Gelbard, H., Benjamini, Y., Heller, R., Nir, Y., et al. (2007). Extrinsic and intrinsic systems in the posterior cortex of the human brain revealed during natural sensory stimulation. *Cerebral Cortex, 17*(4), 766–777.

Greicius, M. D., Srivastava, G., Reiss, A. L., & Menon, V. (2004). Default-mode network activity distinguishes Alzheimer's disease from healthy aging: evidence from functional MRI. *Proceedings of the National Academy of Sciences, 101*(13), 4637–4642.

Grötschel, M., & Holland, O. (1985). Solving matching problems with linear programming. *Mathematical Programming, 33*(3), 243–259.

Guldenmund, P., Demertzi, A., Boveroux, P., Boly, M., Vanhaudenhuyse, A., Bruno, M. A., et al. (2013). Thalamus, brainstem and salience network connectivity changes during propofol-induced sedation and unconsciousness. *Brain Connectivity, 3*(3), 273–285.

Hall, M. A. (1999). *Correlation-based feature selection for machine learning*. Unpublished PhD. Hamilton, NewZealand: The University of Waikato.

He, B. J., Shulman, G. L., Snyder, A. Z., & Corbetta, M. (2007). The role of impaired neuronal communication in neurological disorders. *Current Opinion in Neurology, 20*(6), 655–660.

Heine, L., Soddu, A., Gomez, F., Vanhaudenhuyse, A., Tshibanda, L., Thonnard, M., et al. (2012). Resting state networks and consciousness. Alterations of multiple resting state network connectivity in physiological, pharmacological and pathological consciousness states. *Frontiers in Psychology, 3*, 1–12.

Hoeft, F., Gabrieli, J. D., Whitfield-Gabrieli, S., Haas, B. W., Bammer, R., Menon, V., et al. (2012). Functional brain basis of hypnotizability. *Archives of General Psychiatry, 69*(10), 1064–1072.

Holmes, A., & Friston, K. (1998). Generalisability, random effects and population inference. *NeuroImage, 7*, 754.

Horovitz, S. G., Braun, A. R., Carr, W. S., Picchioni, D., Balkin, T. J., Fukunaga, M., et al. (2009). Decoupling of the brain's default mode network during deep sleep. *Proceedings of the National Academy of Sciences, 106*(27), 11376–11381.

Horovitz, S. G., Fukunaga, M., de Zwart, J. A., van Gelderen, P., Fulton, S. C., Balkin, T. J., et al. (2008). Low frequency BOLD fluctuations during resting wakefulness and light sleep: a simultaneous EEG-fMRI study. *Human Brain Mapping, 29*(6), 671–682.

Kinney, H. C., & Samuels, M. A. (1994). Neuropathology of the persistent vegetative state. *A Review, 53*(6), 548–558.

Laird, A. R., Fox, P. M., Eickhoff, S. B., Turner, J. A., Ray, K. L., McKay, D. R., et al. (2011). Behavioral interpretations of intrinsic connectivity networks. *Journal of Cognitive Neuroscience, 23*(12), 4022–4037.

Laureys, S. (2005). The neural correlate of (un)awareness: lessons from the vegetative state. *Trends in Cognitive Sciences, 9*(12), 556–559.

Laureys, S., Faymonville, M.-E., Degueldre, C., Fiore, G. D., Damas, P., Lambermont, B., et al. (2000). Auditory processing in the vegetative state. *Brain, 123*(8), 1589–1601.

Laureys, S., Goldman, S., Phillips, C., Van Bogaert, P., Aerts, J., Luxen, A., et al. (1999). Impaired effective cortical connectivity in vegetative state: preliminary investigation using PET. *NeuroImage, 9*(4), 377–382.

Laureys, S., Lemaire, C., Maquet, P., Phillips, C., & Franck, G. (1999). Cerebral metabolism during vegetative state and after recovery to consciousness. *Journal of Neurology, Neurosurgery, and Psychiatry, 67*(1), 121.

Laureys, S., Owen, A. M., & Schiff, N. D. (2004). Brain function in coma, vegetative state, and related disorders. *Lancet Neurology, 3*(9), 537–546.

Martuzzi, R., Ramani, R., Qiu, M., Rajeevan, N., & Constable, R. T. (2010). Functional connectivity and alterations in baseline brain state in humans. *NeuroImage, 49*(1), 823–834.

Mason, M. F., Norton, M. I., Van Horn, J. D., Wegner, D. M., Grafton, S. T., & Macrae, C. N. (2007). Wandering minds: the default network and stimulus-independent thought. *Science, 315*(5810), 393–395.

McGeown, W. J., Mazzoni, G., Venneri, A., & Kirsch, I. (2009). Hypnotic induction decreases anterior default mode activity. *Consciousness and Cognition, 18*(4), 848–855.

Norton, L., Hutchison, R. M., Young, G. B., Lee, D. H., Sharpe, M. D., & Mirsattari, S. M. (2012). Disruptions of functional connectivity in the default mode network of comatose patients. *Neurology, 78*(3), 175–181.

Ovadia-Caro, S., Nir, Y., Soddu, A., Ramot, M., Hesselmann, G., Vanhaudenhuyse, A., et al. (2012). Reduction in inter-hemispheric connectivity in disorders of consciousness. *PLoS ONE, 7*(5), e37238.

Raichle, M. E., MacLeod, A. M., Snyder, A. Z., Powers, W. J., Gusnard, D. A., & Shulman, G. L. (2001). A default mode of brain function. *Proceedings of the National Academy of Sciences, 98*(2), 676–682.

Schiff, N. D., Rodriguez-Moreno, D., Kamal, A., Kim, K. H., Giacino, J. T., Plum, F., et al. (2005). fMRI reveals large-scale network activation in minimally conscious patients. *Neurology, 64*(3), 514–523.

Schnakers, C., Majerus, S., Giacino, J. T., Vanhaudenhuyse, A., Bruno, M.-A., Boly, M., et al. (2008). French validation study of the Coma Recovery Scale-Revised (CRS-R). *Brain Injury, 22*(10), 786–792.

Schrouff, J., Perlbarg, V., Boly, M., Marrelec, G., Boveroux, P., Vanhaudenhuyse, A., et al. (2011). Brain functional integration decreases during propofol-induced loss of consciousness. *NeuroImage, 57*(1), 198–205.

Smith, S. M., Fox, P. T., Miller, K. L., Glahn, D. C., Fox, P. M., Mackay, C. E., et al. (2009). Correspondence of the brain's functional architecture during activation and rest. *Proceedings of the National Academy of Sciences, 106*(31), 13040–13045.

Soddu, A., Vanhaudenhuyse, A., Bahri, M. A., Bruno, M.-A., Boly, M., Demertzi, A., et al. (2012). Identifying the default-mode component in spatial IC analyses of patients with disorders of consciousness. *Human Brain Mapping, 33*(4), 778–796.

Soddu, A., Vanhaudenhuyse, A., Demertzi, A., Bruno, M.-A., Tshibanda, L., Di, H., et al. (2011). Resting state activity in patients with disorders of consciousness. *Functional Neurology, 26*(1), 37–43.

Thibaut, A., Bruno, M.-A., Chatelle, C., Gosseries, O., Vanhaudenhuyse, A., Demertzi, A., et al. (2012). Metabolic activity in external and internal awareness networks in severely brain-damaged patients. *Journal of Rehabilitation Medicine, 44*(5), 487–494.

Tian, L., Jiang, T., Liu, Y., Yu, C., Wang, K., Zhou, Y., et al. (2007). The relationship within and between the extrinsic and intrinsic systems indicated by resting state correlational patterns of sensory cortices. *NeuroImage, 36*(3), 684–690.

Turk, D. J., Heatherton, T. F., Macrae, C. N., Kelley, W. M., & Gazzaniga, M. S. (2003). Out of contact, out of mind: the distributed nature of the self. *Annals of the New York Academy of Sciences, 1001*, 65–78.

Van Dijk, K. R. A., Sabuncu, M. R., & Buckner, R. L. (2012). The influence of head motion on intrinsic functional connectivity MRI. *NeuroImage, 59*(1), 431–438.

Vanhaudenhuyse, A., Demertzi, A., Schabus, M., Noirhomme, Q., Bredart, S., Boly, M., et al. (2011). Two distinct neuronal networks mediate the awareness of environment and of self. *Journal of Cognitive Neuroscience, 23*(3), 570–578.

Vanhaudenhuyse, A., Noirhomme, Q., Tshibanda, L. J., Bruno, M.-A., Boveroux, P., Schnakers, C., et al. (2010). Default network connectivity reflects the level of consciousness in non-communicative brain-damaged patients. *Brain, 133*(Pt 1), 161–171.

Ylipaavalniemi, J., & Vigario, R. (2008). Analyzing consistency of independent components: an fMRI illustration. *NeuroImage, 39*(1), 169–180.